

## Differential Cross Sections for $p+p \rightarrow d+\pi^+$ from 1 to 3 BeV

R. M. HEINZ,\* O. E. OVERSETH, D. E. PELLETT†  
*University of Michigan,‡ Ann Arbor, Michigan*

AND

M. L. PERL  
*Stanford University,§ Stanford, California*  
 (Received 4 October 1964)

The differential and total cross sections for the reaction  $p+p \rightarrow d+\pi^+$  have been measured in a counter experiment for incident proton kinetic energies of 1.0, 1.3, 1.5, 1.7, 2.0, 2.5, and 2.8 BeV. Values of the differential cross section are given for barycentric deuteron angles  $\theta$  for  $0 \geq \cos\theta \geq -0.97$  in small intervals of  $\cos\theta$ . From 1.3 to 2.0 BeV, as  $\cos\theta$  varies from  $-0.5$  to  $-1.0$ , the differential cross section rises, passes through a pronounced maximum, and then decreases rapidly. This maximum propagates from  $\cos\theta = -0.8$  at 1.3 BeV to  $\cos\theta = -0.94$  at 2.0 BeV, and evolves into a sharp peak at  $\cos\theta = -1.0$  for energies above 2.0 BeV. The total cross section decreases rapidly and monotonically with energy from  $450 \mu\text{b}$  at 1.0 BeV to  $30 \mu\text{b}$  at 2.8 BeV.

### I. INTRODUCTION

THE primary interest in studying the reaction  $p+p \rightarrow d+\pi^+$  is to provide a test of dynamical models for strong interactions. For example, this reaction is a candidate for proceeding via a one-nucleon exchange mechanism.<sup>1</sup> Or, for another possibility, the reaction might proceed by a one-pion exchange (OPE) with a final-state interaction between the nucleons to form the deuteron.<sup>2,3</sup> Moreover, a statistical model has been proposed<sup>4</sup> which predicts the energy dependence of the differential cross section at  $90^\circ$  for such reactions. Clearly it is desirable to have experimental information on the differential cross sections of such relatively simple two-body reactions in order to evaluate the contribution to the reaction process made by these and other mechanisms.

Another purpose of the experiment was to investigate the behavior of the total cross section for this reaction in this energy region. Previous measurements<sup>5,6</sup> of the differential cross sections near  $0^\circ$  as a function of incident energy had shown a maximum at a c.m. energy of 3.0 BeV. It had been suggested<sup>6</sup> that this maximum might be a manifestation of a diproton resonance. Total cross-section measurements in this energy region were needed to resolve this question.

The reaction  $p+p \rightarrow d+\pi^+$  and its inverse have been extensively investigated below 1 BeV.<sup>7</sup> These studies found that the differential cross section for this reaction rises to a broad maximum at  $\cos\theta = 1.0$  over a considerable range of energies. The total cross section below 1-BeV incident energy is characterized by a narrow maximum at  $E_{\text{c.m.}} = 2.16$  BeV. This behavior has been explained by the excitation of the  $N_{3/2,3/2}^*$  pion-nucleon resonance in an intermediate state of the reaction.

In recent years, several studies of this reaction have been made above 1 BeV. Chapman *et al.*<sup>8</sup> give the differential cross section at  $0.99$  BeV. Turkot *et al.*<sup>5</sup> have measured the differential cross section at  $0^\circ$  for incident proton energies of 1.55, 1.93, 2.11, and 2.50 BeV. Cocconi *et al.*<sup>6</sup> have measured the differential cross section at  $60$  mrad ( $3.5^\circ$ ) in the laboratory for six incident proton energies between 1.35 and 8.0 BeV. Dekkers *et al.*<sup>9</sup> have studied the inverse reaction  $\pi^++d \rightarrow p+p$  for eight energies corresponding to a range of incident proton energies of 1.35–4.0 BeV. This study agrees with our measurements and extends them to higher energy. Total cross sections for the reaction have been reported by Sechi-Zorn<sup>10</sup> at 2 BeV, and by Smith *et al.*<sup>11</sup> at 2.85 BeV. In addition to these measurements, several isolated differential cross-section determinations have been reported: at 10.7 BeV and  $55.7^\circ$ , at 14.1 BeV and  $43.4^\circ$ , and at 22.0 BeV and  $34.7^\circ$ <sup>12</sup>;

\* Present address: Department of Physics, Indiana University, Bloomington, Indiana.

† Present address: Department of Physics, University of California, Davis, Calif.

‡ Supported in part by the Office of Naval Research Contract No. Nonr 1224(23).

§ Supported in part by the U. S. Atomic Energy Commission.  
<sup>1</sup> M. L. Perl, L. W. Jones, and C. C. Ting, Phys. Rev. **132**, 1273 (1963).

<sup>2</sup> T. Yao, Phys. Rev. **134**, B454 (1964).

<sup>3</sup> J. Chahoud, G. Russo, and F. Selleri, Phys. Rev. Letters **11**, 506 (1963).

<sup>4</sup> R. Hagedorn, Nuovo Cimento **35**, 216 (1965).

<sup>5</sup> F. Turkot, G. B. Collins, and T. Fujii, Phys. Rev. Letters **11**, 474 (1963).

<sup>6</sup> G. Cocconi, E. Lillethun, J. P. Scanlon, C. A. Stahlbrandt, C. C. Ting, J. Walters, and A. M. Wetherell, Phys. Letters **7**, 222 (1963).

<sup>7</sup> For references to earlier work on this reaction see Dekkers *et al.*, Ref. 9.

<sup>8</sup> K. R. Chapman, T. W. Jones, Q. H. Khan, J. S. McKee, H. B. Van Der Raay, and Y. Tanimura, Phys. Letters **11**, 253 (1964).

<sup>9</sup> D. Dekkers, B. Jordan, R. Mermod, C. C. Ting, G. Weber, T. R. Willitts, K. Winter, X. DeBouard, and M. Vivargent, Phys. Letters **11**, 161 (1964).

<sup>10</sup> B. Sechi-Zorn, Bull. Am. Phys. Soc. **7**, 349 (1962).

<sup>11</sup> G. A. Smith, H. Courant, E. C. Fowler, H. Kraybill, J. Sandweiss, and H. Taft, Phys. Rev. **123**, 2160 (1961).

<sup>12</sup> W. F. Baker, E. W. Jenkins, A. L. Read, A. D. Krisch, J. Orear, R. Rubenstein, D. B. Scarf, and B. T. Ulrich, Phys. Rev. **136**, B779 (1963).

at 2.4 BeV and  $0^\circ$ <sup>13</sup>; at 11.5 BeV and  $0^\circ$ <sup>14</sup>; and at 4.1 BeV and  $90^\circ$ <sup>15</sup>

In the experiment reported here, the differential and total cross sections were measured for the reaction  $p+p \rightarrow d+\pi^+$  for seven energies of the incident protons between 1.0 and 2.8 BeV. Preliminary results for six of the energies have been published elsewhere.<sup>16</sup>

## II. EXPERIMENTAL ARRANGEMENT AND PROCEDURE

The measurements were made in a scintillation-counter experiment run in an external proton beam of the Brookhaven Cosmotron. Desired events, which comprise 0.05–0.5% of the total  $pp$  cross section in this energy interval, were recorded when a coincidence occurred between the pion-counter telescope and the deuteron-counter telescope mounted on a spectrometer for momentum analysis and time-of-flight selection.

### A. External Beam

An external proton beam was designed for the Cosmotron to be an intense, well collimated beam to an open experimental area. The beam at the target had a spot size of about 1 or 1.5 in. in diam, depending on the beam energy, and an angular divergence of about  $0.1^\circ$  in both horizontal and vertical planes.

Two direct methods were used to determine the energy of the beam. These were: (1) measuring the Cosmotron magnetic field strength and radius of the circulating beam at ejection, and (2) measuring the frequency and orbital path length of the internal beam at ejection. These determinations typically agreed to  $\pm 0.05$  BeV.

The beam intensity was set as high as possible subject to the requirement that the accidental counting rate be less than 10% of the rate for actual events and that no counter have a singles counting rate greater than 1 Mc/sec. The beam intensity varied from  $2 \times 10^8$  to  $8 \times 10^8$  protons/pulse.

The beam was incident on a hydrogen target 3 in. long and 4 in. in diam. Emerging pions and deuterons passed through a 0.015-in. Mylar window with no obstructing supports.

### B. Counter Telescopes and Spectrometer

A diagram of the experimental layout is shown in Fig. 1. The sizes of the counters are given in Table I. The first counter of the pion telescope,  $\pi_1$ , defined the solid angle, which varied from 0.035 to 0.87 msr, de-

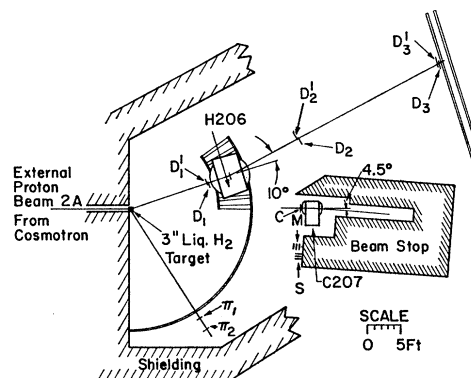


FIG. 1. The experimental arrangement.

pending on which of the two  $\pi_1$  counters was used and its distance from the target. This distance, which varied from 8 to 20 ft, could be changed by sliding the carriage upon which the  $\pi$  counters were mounted radially along a 6-in. wide-flanged beam. The angle between the pion telescope and the beam line was varied by rotating the wide-flanged beam, which pivoted on a post mounted directly underneath the target and rolled on a circular rail located 19 ft from the target. The pion angle, as well as the deuteron angle, was determined quantitatively by calibrating a scale, mounted on this rail, using a transit secured to the top of the pivot post.

The deuteron was detected by two overlapping counter telescopes, consisting of three counters each, and momentum analyzed by an 18-in.  $\times$  36-in. bending magnet H206, which deflected the deuterons by  $\pm 10^\circ$ . This magnet had a 10.5-in. separation between the pole faces. In Fig. 1, the two deuteron counter channels are labeled  $D_1, D_2, D_3$  and  $D_1', D_2', D_3'$ . The 40-ft flight path between the  $D_1$  and  $D_3$  counter provided time-of-flight selection. The combined effects of the time-of-flight selection and momentum analysis in this spectrometer separated the deuterons from pions and protons for momenta up to 2.4 BeV/c. Because the initial state of this reaction consists of identical particles, the differential cross section is symmetric about  $90^\circ$  in the c.m. system and it was only necessary to measure it for deuterons going backward in the c.m. system, where this momentum condition is satisfied.

TABLE I. Scintillation counter sizes.

Counter	Size width $\times$ height (in.)	Thick- ness (in.)
$\pi_1$	4 $\times$ 2 or 2 $\times$ 1	$\frac{1}{2}$ $\frac{1}{2}$
$\pi_2$	7.5 $\times$ 4	$\frac{1}{2}$
$D_1, D_1'$	5.5 $\times$ 8	$\frac{1}{2}$
$D_2, D_2'$	13 $\times$ 19	$\frac{3}{8}$
$D_3, D_3'$	17 $\times$ 30	$\frac{1}{2}$
C	8 (diam)	$\frac{1}{2}$
M (3 counters)	1 $\times$ 1	$\frac{1}{4}$
S (3 counters)	1.5 $\times$ 1.5	$\frac{3}{8}$

<sup>13</sup> N. W. Reay, A. C. Melissinos, J. T. Reed, T. Yamanouchi, and L. C. L. Yuan, Phys. Rev. **142**, 918 (1966).

<sup>14</sup> R. C. Lamb, R. A. Lundy, T. B. Novey, D. D. Yovanovich, and R. Lander, Phys. Rev. Letters **17**, 100 (1966).

<sup>15</sup> K. Ruddick, L. G. Ratner, K. W. Edwards, C. W. Akerlof, R. H. Hiebler, and A. D. Krisch, Phys. Rev. **165**, 1442 (1968).

<sup>16</sup> O. E. Overseth, R. M. Heinz, L. W. Jones, M. J. Longo, D. E. Pellett, M. L. Perl, and F. Martin, Phys. Rev. Letters **13**, 59 (1964).

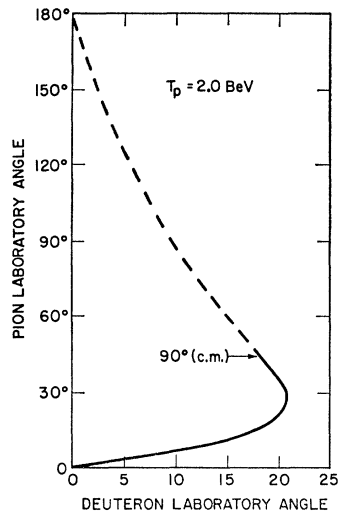


FIG. 2. Kinematics curve for the reaction  $p+p \rightarrow d+\pi^+$  at an incident proton energy of 2.0 BeV. The solid line represents the region where the cross sections were measured in this experiment, and corresponds to deuterons going backward in the barycentric system.

This region is shown in Fig. 2 for an incident energy of 2.0 BeV. Two deuteron channels were used to increase the momentum resolution of the spectrometer. Unequal counting rates in these two channels indicated that the apparatus was not set at the proper kinematic angles or that the beam energy was incorrect.

The deuteron telescope angle was varied by moving the magnet, which was mounted on a motorized carriage, along the arc of a circle on railroad tracks, a portion of which is shown in Fig. 1. The D1 and D2 counters were attached to the magnet carriage, while the D3 counter could be moved along a pair of parallel I-beams. The magnet and positioning of D3 counters were calibrated by using the standard wire-orbit technique.

It was possible to reduce the size of the D3 counters by approximately 20% by taking advantage of kinematical focusing. If  $p$  and  $\varphi$  are the laboratory momentum and angle of the deuteron, respectively, then  $dp/d\varphi > 0$  as  $\varphi$  goes from  $0^\circ$  to its maximum, for deuterons backward in the c.m. system (see Fig. 2), and then  $dp/d\varphi < 0$ . If  $\alpha$  is the angle between the deuterons leaving magnet H206 (see Fig. 1) and the beam, then

$$\alpha = \varphi \pm LeB/p,$$

where  $L$  is the length of the magnet,  $B$  is the magnetic field, and  $e$  is the deuteron charge. The plus sign is for counterclockwise bending (as seen from above) and the minus sign is for clockwise bending. The deuterons emerge from the magnet within some range of angles  $\Delta\alpha$ , where

$$\Delta\alpha = \Delta\varphi [1 \mp LeB\Delta p/p^2\Delta\varphi].$$

$\Delta\alpha$  is obviously smaller for a counterclockwise bend when  $dp/d\varphi > 0$  and for a clockwise bend when  $dp/d\varphi < 0$ .

$< 0$ , since  $LeB/p^2$  is always greater than zero. In this experiment, the direction of bend was always chosen to minimize  $\Delta\alpha$ .

The sizes of the deuteron counters were determined by a computer program which, using ray-tracing techniques, considered the effects of beam size and angular divergence,  $\pi$ 1 size and distance from the target, the length of the target, multiple Coulomb scattering, and kinematical focusing. The amount of overlap between pairs of deuteron counters was determined primarily by considering the Coulomb scattering of the deuterons.

The kinematics of the reaction are such that it was possible to measure all barycentric deuteron angles  $\theta$  for  $0 \geq \cos\theta \geq -0.96$  or  $-0.97$  (depending on beam energy) by varying the  $\pi$  telescope from  $5^\circ$  to  $58^\circ$  and the deuteron telescope from  $6.7^\circ$  to  $23^\circ$ . At small laboratory deuteron angles, the beam struck the yoke of the H206 magnet and it was necessary to reduce the beam intensity, so that the singles counting rates in the D1 counters would not be too large.

After traversing the open experimental area, the beam entered an iron and concrete beam stop. In order to accommodate small-angle clockwise bends of the deuterons, the beam dump was cocked at an angle with the beam line and magnet C207 steered the beam into the beam dump. At the beginning of the experiment, the beam was contained in a vacuum pipe or helium bag after passing through the hydrogen target, but when it was shown that this precaution did not affect the background accidentals rate, they were dispensed with.

### C. Monitor Counters

The beam was monitored by two sets of scintillation-counter telescopes, each comprised of three counters. The M monitor telescope, used to normalize the measured cross sections, was pointed toward the target at a laboratory angle of  $11.3^\circ$ , while the S telescope was aligned so that it looked at counter C (see Fig. 1). C was an in-beam counter used to monitor the beam structure and beam drift off the beam line. It also served as a source of particles for S which essentially depended only on the incident beam intensity and not upon whether the target was full or empty, since less than 2% of the beam interacted in the liquid hydrogen.

### D. Normalization

The monitor counters M were calibrated by measuring the  $C^{11}$  activity induced by the beam in 0.004-in.-thick polyethylene foil by means of the reaction  $C^{12}(p,pn)C^{11}$ . The foil was mounted on the downstream end of the target assembly and irradiated for 1 min by a beam with an approximate intensity of  $2-5 \times 10^9$  particles/pulse. The  $C^{11}$  activity was then measured in a calibrated NaI well-counter by detecting the  $\gamma$  rays resulting from the annihilation of the positrons emitted by the  $C^{11}$  atoms. The cross sections for this reaction in this energy region have been given by Poskanzer

*et al.*<sup>17</sup> and by Cumming *et al.*, and the correction necessary to include the effect of recoiling  $C^{11}$  atoms breaking chemical bonds and diffusing out of the foil gas been given by Cumming *et al.*<sup>18</sup>

This allowed the determination of  $F/M$  at each energy, where  $M$  is the number of coincidences in the monitor counters when the foil was irradiated by  $F$  protons. The error in the normalization calibration was  $\pm 8\%$  due to combination of the uncertainty in cross section for forming  $C^{11}$ , the calibration of the well counter, and counting statistics in determining the activity of the  $C^{11}$  in the foil. For most energies, two foils were irradiated and the resulting  $F/M$  values always agreed to within  $3\%$ .

### E. Electronics

Standard fast-electronic circuitry was used. Counters  $\pi 1$  and  $\pi 2$  formed  $\pi$  coincidence with an anticoincidence counter in front of the light pipe of  $\pi 1$ . D1, D2, and D3 formed D coincidence and D1', D2', and D3' formed D' coincidence. An event was a  $\pi D$  coincidence between the  $\pi$  telescope and either (or both) of the deuteron telescopes. Singles rates and all coincident rates were also monitored.

Before the experiment all of the scintillation counters were plateaued and the characteristic time delay between the incidence of a particle and the output pulse from the photomultiplier tubes was determined with a light pulser. During the experiment these delays were checked by running time-of-flight delay curves on protons from elastic scattering. With this information, it was possible to calculate the proper delay cables to insert between the counters and coincidence circuits for the  $\pi^+d$  final state. Both D3 counters had a phototube on each end to decrease the timing jitter and increase the signal-to-noise ratio from these counters.

### F. Experimental Checks

Numerous checks were made to verify that the events detected indeed corresponded to the  $\pi^+d$  final state. Deuteron time-of-flight delay curves, obtained by varying the delay between the  $\pi$  and D coincidence circuits, resulted in yield-versus-delay curves which typically had a flat top of width 7 nsec, a full width at half-maximum of 10 nsec, and a full width for a 10% yield of 16 nsec. These curves were centered about the delay corresponding to the  $\pi^+d$  final state. Curves of yield versus the current in magnet H206 similarly had a maximum at the current corresponding to the momentum of the deuteron from the  $\pi^+d$  final state. Angular-correlation measurements, obtained by fixing the deuteron (pion) angle and finding the yield as a

function of pion (deuteron) angle also identified the  $\pi^+d$  final state. A curve of yield versus pulse length in the deuteron channels was run to insure that no events were lost because of the spread in deuteron flight time being of the order of the time resolution of the coincidence circuit. Finally, for low beam energies it was possible to measure the differential cross section at forward barycentric deuteron angles and verify the symmetry of the reaction about  $90^\circ$ .

## III. DATA CORRECTIONS

This section describes the corrections which were applied to the data.

### A. Nuclear Interactions

Some of the desired events were not recorded because the pion and/or the deuteron did not travel completely through their respective telescopes because of nuclear interactions in the hydrogen target, air, or scintillators. The number of events lost in this manner can be calculated if the relevant cross sections are known. A good approximation to the cross sections is given by  $\sigma_{dA} = \sigma_{dN} A^{2/3}$ , where  $\sigma_{dN}$ , the deuteron-nucleon total cross section, is approximately 80 mb.<sup>19</sup> Similarly,  $\sigma_{\pi A} = \sigma_{\pi N} A^{2/3}$ , where  $\sigma_{\pi N} = 35$  mb.<sup>20</sup>

### B. Multiple Coulomb Scattering

The deuteron counters were made large enough to prevent any loss of events due to multiple Coulomb scattering of the deuterons. Events in which the pion was scattered and did not go through the solid-angle-defining counter ( $\pi 1$  in Fig. 1) were compensated for by events in which the pion scattered into  $\pi 1$ , since the deuteron counters were large enough to detect the deuterons corresponding to these pions.

It was possible to verify experimentally that there was a negligible loss of events due to multiple Coulomb scattering in the following manner: At one pion angle at each energy, the differential cross section was measured twice, once using a pion counter which subtended the designed solid angle and once with a solid angle  $\frac{1}{4}$  as large. If the deuteron counter telescopes were not large enough to collect all of the desired deuterons, the yield would be higher with the smaller pion solid angle, since then the deuterons would be confined to a smaller solid angle. There was no statistically significant difference between the two measurements.

### C. Decay of Pions

The variable pion path length, which had a maximum value of 22 ft, required a maximum of 4.5 nsec flight time (in the pion barycentric system). As many as

<sup>17</sup> A. M. Poskanzer, L. P. Remsberg, S. Katcoff, and J. B. Cumming, Phys. Rev. **133**, B1507 (1964); J. B. Cumming, G. Friedlander, and C. E. Swartz, *ibid.* **111**, 1386 (1958).

<sup>18</sup> J. B. Cumming, A. M. Poskanzer, and J. Hudis, Phys. Rev. Letters **6**, 484 (1961); J. B. Cumming, J. Hudis, A. M. Poskanzer, and S. Kaufman, Phys. Rev. **128**, 2392 (1962).

<sup>19</sup> F. F. Chen, C. P. Leavitt, and A. M. Shapiro, Phys. Rev. **103**, 211 (1956).

<sup>20</sup> V. S. Barashenkov, Ob'edinennyi, Institut Yadernykh Issledovaniy Report (unpublished).

16% of the pions decayed before reaching the final counter. However, the muons were emitted by the highly relativistic pions in a narrow forward cone with a maximum half-angle of  $3.0^\circ$  in the laboratory. Thus the coincidence was completed in many cases by the muon. Those events in which the muon missed the pion counters were compensated for by events in which pions were slightly off angle being counted by decaying and sending a muon through the counter system.

Verification that the number of events lost by pion decay was not significant was done empirically by re-measuring one point with a 50% shorter pion travel length. There was no statistically significant difference in the two resulting cross sections.

#### D. Accidental Coincidences

Accidental events, in which independent pulses from the pion and deuteron channels occur by chance within a short time interval and are counted by the coincidence circuit, were indicated by recording the coincidences between the two channels when they were 31 nsec out of time. These accidental coincidences were recorded throughout the experiment. By adjusting the beam intensity, the accidentals were always held to less than 10% of the good events. However, the shape of the time distribution of the beam, which could not be controlled by the experimenters, was much more influential in causing accidentals than was the beam intensity.

#### E. Background Events from Target

When the liquid hydrogen was emptied from the target, the number of events recorded was approximately 2.7% of the number of events with a full target for the same amount of incident beam. Only about 0.1% of this was due to the hydrogen vapor which remained in the empty target, resulting in a 2.6% correction to the data.

#### F. Beam Attenuation

Since part of the beam interacts in passing through the target, the downstream end of the target only sees some fraction of the initial beam flux. This effect can be corrected by using an effective target length  $L_{\text{eff}}$ , which is defined by

$$I(0)L_{\text{eff}} = \int_0^L I(x)dx,$$

where  $L$  is the actual target length and  $I(x)$  is the number of protons per pulse which pass through  $x$ , the  $x$  axis pointing along the beam direction with its origin at the upstream edge of the target. The resulting expression  $L_{\text{eff}}$  is

$$L_{\text{eff}} \approx L(1 - \frac{1}{2}\sigma\rho L),$$

where  $\sigma$  is the total  $pp$  cross section and  $\rho$  is the number of protons/cm<sup>3</sup> in the target.

#### G. Beam Energy

The energy of the beam could be determined with an accuracy of about  $\pm 0.05$  BeV. In addition to the fact that the energy at which the cross section is measured is unknown by this amount, there is an error introduced of approximately  $\pm 2\%$  in transforming the measured laboratory cross sections to the barycentric cross sections, since the Jacobian for a given laboratory angle is a function of the beam energy. This effect, of course, cannot be corrected for.

#### H. Counter Efficiency

Because of the small size and relatively large thickness of the  $\pi$  counters and the D1 counters (see Table I), it is assumed that they were essentially 100% efficient. The efficiencies of the D2 and D3 counters were not measured, but were estimated to be  $99 \pm 1\%$  because of the moderate size of the D2's and the fact that each D3 counter had two phototubes. The dead-time correction for the counters was 3%.

### IV. RESULTS

The following formula was used to calculate the differential cross sections:

$$\frac{d\sigma}{d\Omega} = \frac{N(\pi D) - N(\pi \bar{D})}{\rho(F/M)MLJ(\Delta\Omega)} \alpha\beta\gamma\delta\epsilon\zeta,$$

where  $N(\pi D)$  is the total number of events at a given angle;  $N(\pi \bar{D})$  is the total number of accidental events at a given angle;  $\rho$  is the density of liquid hydrogen,  $4.23 \times 10^{22}$  protons/cc;  $F/M$  is the normalization factor for M monitor telescope, typically  $3 \times 10^6$ ;  $M$  is the number of coincidences in M telescope;  $L$  is the length of hydrogen target (3.03 in.) when filled with liquid hydrogen and surrounded by vacuum;  $\Delta\Omega$  is the solid angle subtended by  $\pi 1$  counter in the laboratory;  $J$  is the Jacobian which transforms solid angle ( $\Delta\Omega$ ) from laboratory to c.m. system;  $\alpha$  is the correction for nuclear interactions ( $= 1.13 \pm 0.03$ );  $\beta$  is the correction for multiple Coulomb scattering loss ( $= 1.01 \pm 0.01$ );  $\gamma$  is the correction for background events ( $= 0.974 \pm 0.05$ );  $\delta$  is the beam attenuation correction ( $= 1.01$ );  $\epsilon$  is the correction for counter dead time ( $= 1.03 \pm 0.03$ );  $\zeta$  is the correction for counter efficiency ( $= 1.02 \pm 0.02$ );  $\alpha\beta\gamma\delta\epsilon\zeta$  is the total correction ( $= 1.18 \pm 0.05$ ).

The errors stated in the corrections applied above are estimated. When combined orthogonally with the Jacobian error of  $\pm 2\%$  due to the uncertainty of the beam energy and the normalization error of  $\pm 8\%$ , the net nonstatistical error is  $\pm 10\%$ . The statistical error ranged from about  $\pm 5$  to  $\pm 15\%$ , but was usually about  $\pm 7\%$ .

The results for the differential cross sections are presented in Table II and displayed in Fig. 3, where the errors indicate the standard deviations from counting

TABLE II. Differential and total cross sections for the reaction  $p+p \rightarrow d+\pi^+$ .<sup>a</sup>

$\cos\theta$ (c.m.)	$T_p$ (BeV):		$d\sigma/d\Omega, \mu\text{b}/\text{sr}$ (c.m.)						
	$E^*$ (BeV):		1.0	1.3	1.5	1.7	2.0	2.5	2.8
			2.3	2.4	2.5	2.6	2.7	2.9	3.0
-0.97								12.3±1.2	12.8±2.3
-0.965					9.9±0.8	10.6±0.9	9.5±0.7		
-0.96	50.1±2.5								
-0.95		17.5±1.3			12.1±0.7	12.5±0.9		10.6±0.8	8.3±0.5
-0.94							8.3±0.6		
-0.93	49.9±2.7								
-0.925		22.7±1.6		14.6±1.0	14.6±0.7			6.4±1.0	
-0.92							10.2±0.7		
-0.90	52.1±2.0	21.0±0.8	15.9±0.6	16.1±0.8	16.1±0.8	10.0±0.5	5.7±0.4	5.1±0.4	
-0.85		24.2±1.1	16.4±0.6	12.9±0.9	8.4±0.5			3.7±0.3	
-0.80	51.2±2.4	25.0±0.9	13.3±0.8	11.9±0.8	7.3±0.4	3.5±0.2		3.3±0.3	
-0.70	45.9±2.2	23.8±0.8	13.1±0.7	9.4±0.5	6.2±0.3	2.7±0.3		2.2±0.2	
-0.60	42.1±1.5	20.1±0.7	10.2±0.5	6.0±0.4	4.7±0.3	1.9±0.2		1.7±0.2	
-0.50	33.4±1.7	17.8±0.9	9.7±0.5	5.0±0.3	2.9±0.2	1.4±0.1		1.2±0.1	
-0.40	31.9±1.6	14.5±0.7	7.6±0.3	4.4±0.2	2.4±0.1			1.0±0.1	
-0.30	24.4±1.2	13.6±0.7	8.6±0.5	3.8±0.2			0.7±0.1		
-0.20	23.5±1.1	12.4±0.6	6.9±0.5	3.1±0.2		1.3±0.1			
-0.10	21.0±0.9	13.0±0.7	6.2±0.4	3.0±0.2		1.2±0.1		0.8±0.1	
0	20.3±0.9	12.2±0.6	6.3±0.4	2.9±0.2		1.1±0.1			
$\sigma_{\text{tot}}$ ( $\mu\text{b}$ )	452±21	217±11	123±7	84±5	53±3	33±3		33±3	30±3

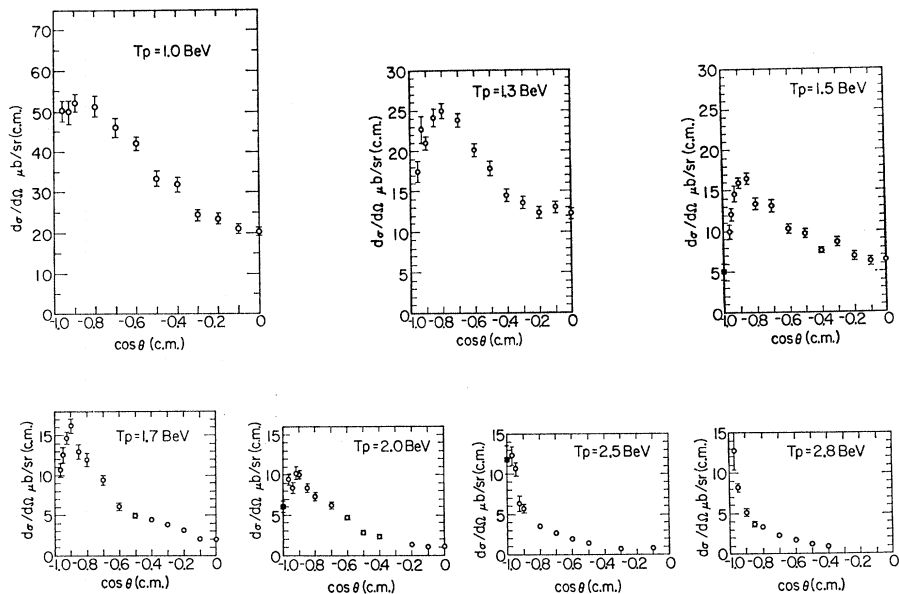
<sup>a</sup> ( $T_p$  is the kinetic energy of the incident proton.  $E^*$  is the total energy in the c.m. system.  $\theta$  is the c.m. angle of the deuteron relative to the direction of the incident proton.)

statistics. The  $0^\circ$  data of Turkot are also plotted for those energies which both experiments covered. The 1.0-BeV data can be compared with the results of Chapman *et al.*,<sup>8</sup> and the agreement is very good. Higher-energy data can be compared with the results of Dekkers *et al.*,<sup>9</sup> who studied the reaction  $\pi^+ + d \rightarrow p + p$  for a range of  $\pi^+$  energies which correspond to incident proton energies from 1.35 to 3.9 BeV for the inverse reaction. Employing the principle of detailed balancing, these cross sections can be translated to those for the inverse reaction, and the agreement between the two experiments is very good. As an example,

in Fig. 4 the results of Dekkers *et al.* are compared with ours at 2.8 BeV.

The total cross sections are also given in Table II. They were obtained by fitting the differential cross sections with a series of even powers of  $\cos\theta$ , using a weighted least-squares method, and integrating the resulting expression analytically. In Fig. 5 they are plotted along with data of others showing the behavior of the total cross section for this reaction as a function of total c.m. energy. This graph corresponds to incident proton energies from 500 MeV to 4 BeV. In addition to measurements above 1 BeV already referred to, the

FIG. 3. Differential cross sections in the c.m. system for the reaction  $p+p \rightarrow d+\pi^+$  in  $\mu\text{b}/\text{sr}$  plotted versus  $\cos\theta$  of the deuteron (in the c.m. system). The  $0^\circ$  data from Ref. 5 are indicated by solid squares.



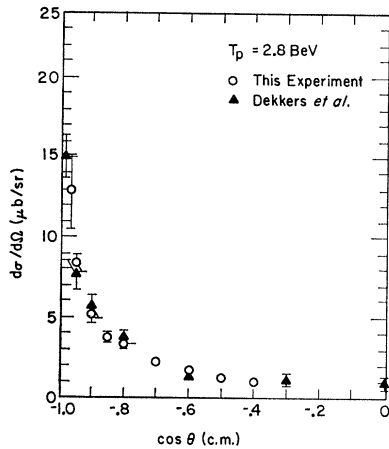


FIG. 4. Comparison of the results of this experiment at 2.8 BeV with the results of Dekkers *et al.* for the inverse reaction  $\pi^+ + d \rightarrow p + p$ .

graph contains lower-energy data of Neganov and Parfenov<sup>21</sup> and of Meshcheryachov *et al.*<sup>22</sup> There is good agreement among the various experiments.

## V. DISCUSSION

The differential cross section for this reaction at 1.0 BeV shows a behavior typical of lower-energy data.

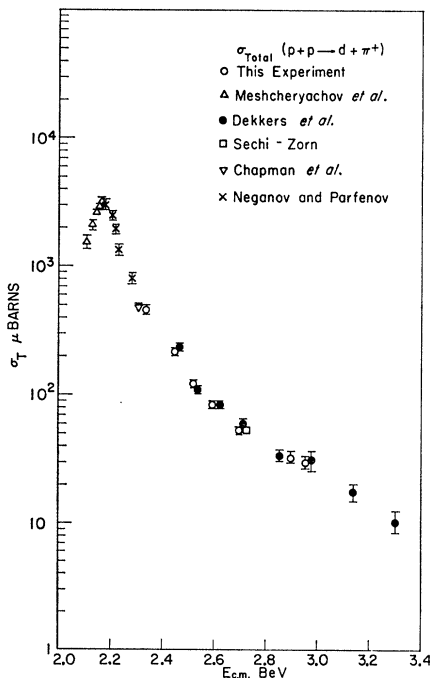


FIG. 5. Total cross sections for the reaction  $p + p \rightarrow d + \pi^+$  in  $\mu\text{b}$  plotted as a function of  $E_{c.m.}$ , the total energy in the c.m. system.

<sup>21</sup> B. S. Neganov and L. B. Perfenov, Zh. Experim. i Teor. Fiz. 34, 767 (1958) [English transl.: Soviet Phys.—JETP 7, 528 (1958)].

<sup>22</sup> M. G. Meshcheryachov, B. S. Neganov, N. P. Bogachev, and

The cross section rises to a broad maximum at  $0^\circ$  (and  $180^\circ$ ). However, at higher energies a new and different type of behavior appears. From 1.3 to 2.0 BeV, as  $\cos\theta$  varies from  $-0.5$  to  $-1.0$ , the differential cross section rises, passes through a pronounced maximum, and then decreases rapidly. This maximum propagates from  $\cos\theta = -0.8$  at 1.3 BeV to  $\cos\theta = -0.94$  at 2.0 BeV, and evolves into a sharp peak at  $\cos\theta = -1.0$  for energies above 2.0 BeV.

These general features of the differential cross section can be understood in terms of a one-nucleon exchange model for the reaction.<sup>23</sup> If a deuteron wavefunction corresponding to a strong, repulsive core in the nucleon-nucleon potential is used to calculate the neutron-proton-deuteron vertex function, the result is a function which causes a maximum in the differential cross section. This maximum moves towards  $\cos\theta = -1.0$  as the incident energy increases. Although this model gives the qualitative features of the data, the over-all agreement is rather poor. This is not surprising, since the exchange neutron is far from the mass shell (which casts some doubt on a peripheral model calculation), a nonrelativistic deuteron wave function was used, and it is not totally clear how to include the effects of absorption in the calculations.

The OPE calculation is complicated by the presence of a loop integral. Yao<sup>2</sup> has evaluated the Feynman diagram, making several important assumptions and approximations. Agreement between the model and the data from this experiment is not good, although the normalization is approximately correct—even though no absorption has been included. There is no mechanism in this OPE calculation for a differential cross-section maximum which systematically shifts with increasing energy, as is observed.

In the BeV region the total cross section decreases rapidly and monotonically. There is no evidence of strong resonant behavior beyond the maximum at  $E_{c.m.} = 2.16$  BeV. The maximum previously found at 3.0 BeV by combining forward differential cross section data<sup>5,6</sup> of several experiments does not appear to be a reflection of a maximum in the total cross section but rather is caused by the unusual behavior of the cross sections near  $0^\circ$  in this region.

In lieu of a good theory for strong interactions it has become commonplace, especially for elastic scattering, to attempt to fit the data over a large range of energies by simple expressions involving one or two variables such as c.m. energy or momentum transfer. It is hoped that such parametrization, if successful, would provide clues as to the form of the interaction or mechanism operative, as well as provide a good basis for interpolation and extrapolation from existing data. In this spirit

V. M. Sidorov, Dokl. Adad. Nauk SSSR 100, 673 (1955); M. G. Meshcheryachov and B. S. Neganov, *ibid.* 100, 677 (1955).

<sup>23</sup> R. M. Heinz, O. E. Overseth, and M. H. Ross, Bull. Am. Phys. Soc. 10, 19 (1965); J. Mathews and B. Deo, Phys. Rev. 143, 1340 (1966).

we present two parametrizations of the results of the data on this reaction.

Hagedorn<sup>4</sup> has extended the statistical model which described proton-proton elastic scattering near  $90^\circ$  to include a prediction for the behavior of large-angle cross sections for all reactions of the type  $p+p \rightarrow A+B$ . According to this model, the large-angle (near  $90^\circ$ ) cross sections for such reactions should decrease with increasing c.m. energy as  $\exp[-3.30E_{c.m.}]$ , where  $E_{c.m.}$  is the c.m. energy in BeV. In Fig. 6 is plotted the  $90^\circ$  cross section as given by the data from this experiment plus the two highest energy measurements of Dekkers *et al.* and the recent measurement of Ruddick *et al.* Although the energies involved here may be too low for the statistical model to be applicable, the data appear to have approximately such exponential behavior, but with a slope twice that given by Hagedorn.

It is interesting to investigate the dependence of the cross section for this reaction on the momentum transfer. In Fig. 7 are plotted the differential cross sections against the square of the transverse momentum  $P_\perp$  in the c.m. system. In order to remove the energy dependence of the reaction, each point has been normalized to the  $0^\circ$  cross section for that energy, where  $P_\perp=0$ . Data have been plotted for energies greater than 2.5 BeV where the differential cross section no longer turns over before  $0^\circ$ . The values of the cross section at  $0^\circ$  used for this plot were  $12 \pm 1.2$ ,  $14 \pm 1.4$ ,  $8 \pm 0.8$ ,  $6 \pm 0.6$ ,  $5.5 \pm 0.5$ ,  $3.1 \pm 1.0$ , and  $2.7 \pm 1.0$   $\mu\text{b}/\text{sr}$  for incident en-

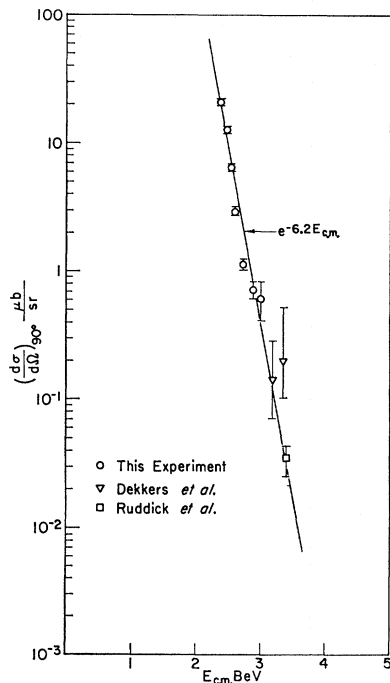


FIG. 6. Differential cross section at  $90^\circ$  for the reaction  $p+p \rightarrow d+\pi^+$  plotted versus the total energy in the c.m. system. The data plotted here cover a range of incident proton energies from 1.0 to 4.1 BeV.

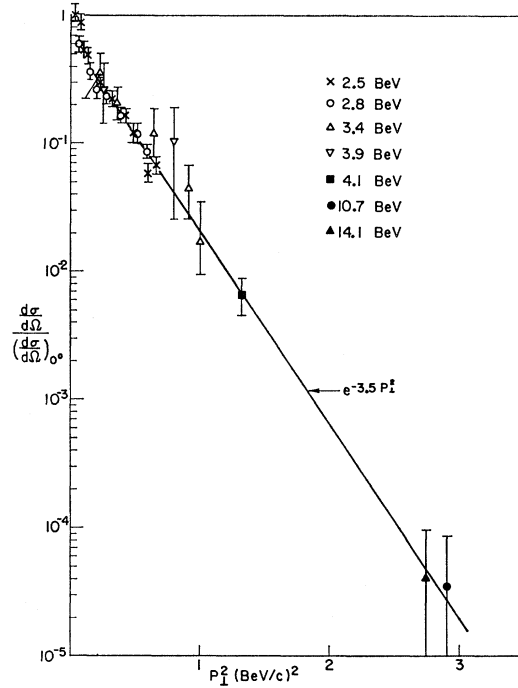


FIG. 7. Plot of the cross section for the reaction  $p+p \rightarrow d+\pi^+$ . The ratio of  $d\sigma/d\Omega$  to  $d\sigma/d\Omega$  at  $0^\circ$  is plotted against the transverse momentum squared. Data at 2.5 and 2.8 BeV are from this experiment, at 3.4 and 3.9 BeV from Ref. 9, at 4.1 BeV from Ref. 15, and at 10.7 and 14.1 BeV from Ref. 12.

ergies of 2.5, 2.8, 3.4, 3.9, 4.1, 10.7, and 14.1 BeV, respectively.<sup>24</sup> It appears that the differential cross sections for this reaction are given fairly well by

$$\frac{d\sigma}{d\Omega} = \left( \frac{d\sigma}{d\Omega} \right)_{0^\circ} A \exp(-3.5P_\perp^2)$$

over a considerable range of energies for  $P_\perp^2 > 0.15$ . Note that this slope,  $3.5 (\text{BeV}/c)^{-2}$ , is the slope characteristic of the production process of  $\pi$  mesons by protons on protons, as found by Ratner *et al.*<sup>25</sup> Slopes characterizing elastic scattering processes are typically twice this value for comparable momenta transfer.

#### ACKNOWLEDGMENTS

It is a pleasure to thank L. W. Jones and M. J. Longo for their strong support throughout all phases of the experiment and F. Martin for his help in the design of the experiment. The assistance of J. Harris, W. Merkle, and the entire Cosmotron staff was greatly appreciated. We also would like to thank Brookhaven National Laboratory for its hospitality.

<sup>24</sup> The values for incident energies less than 4.1 BeV come from extrapolation to  $0^\circ$  of the differential cross-section data at each energy. The  $0^\circ$  cross sections for the two highest energies were obtained from interpolation between the extrapolated values for the lower energies and the  $0^\circ$  measurement of Ref. 14 at 11.5 BeV.

<sup>25</sup> L. G. Ratner, K. W. Edwards, C. W. Akerlof, D. G. Crabb, J. L. Day, A. D. Krisch, and M. T. Lin, Phys. Rev. Letters **18**, 1218 (1967).